# 3D DYNAMIC INTERACTION OF CRACKS UNDER IMPACT LOADING

D. GROSS and B. CHEN
*Institute of Mechanics, Technische Hochschule Darmstadt*
*D-64289 Darmstadt, Germany*

## ABSTRACT

3D Dynamic interaction of two circular cracks in an infinite medium under impact loading is investigated. A time-domain boundary integral equation method is used for calculating the time dependence of crack opening displacements and subsequently the dynamic stress intensity factors. Numerical results are presented for various crack configurations including the macrocrack-microcrack interaction problem.

## KEYWORDS

Dynamic K-factors, 3D problems, crack interaction

## INTRODUCTION

Most of all investigations on the dynamic behavior of stationary cracks are concentrated on 2D problems. Recently more attention has been paid to the 3D respose of cracks to dynamic loading. One reason for this is the development of suitable experimental and numerical methods combined with the increasing computer power. Another is the necessity of 3D investigations for a detailed understanding of the dynamic failure behavior of cracked structures. As examples, 3D-FEM studies of test specimen under dynamic load have been carried out by Zehnder and Rosakis (1990) and Aoki and Kimura (1993), partly in order to get an insight in effects such as the so-called incubation time. Other papers are concerned with the fundamental problem of cracks in an infinite region (Chen and Sih, 1977; Shindo, 1984; Sládek and Sládek, 1986; Hirose and Achenbach, 1989; Zhang, 1991; Zhang and Gross, 1993a,b; Xiao et al., 1995; Wen et al., 1996). In these investigations only a single crack of a circular, rectangular or elliptic shape under dynamic loading is considered.

Interaction of several or many cracks is of considerable importance for certain applications in fracture mechanics as well as for the constitutive behavior of solids like rock,

ceramics or concrete. For the corresponding 2D problem a number of solutions exist for the static and the dynamic case. Three dimensional crack interaction problems usually are regarded as difficult and therefore only a few solutions are available for the static case. They are concentrated on the interaction of two penny or ellipse-shaped cracks (Isida et al., 1985; Fabrikant, 1987; Kachanov and Laures, 1989) and of penny-shaped cracks with the straight front of a semiinfinite crack (Laures and Kachanov, 1991; Huang and Karihaloo, 1993). Till now, to our knowledge, no investigation on the 3D response of multiple cracks to transient loading has been available in the literature.

In this paper the response of two parallel circular cracks embedded in an infinite elastic solid under the action of impact loading is investigated using a non-hypersingular time-domain boundary integral equation (BIE) method developed by Zhang (1991). The BIE is solved numerically via a collocation method in conjunction with a time-stepping scheme. The time-dependend dynamic stress intensity factors are determined for various crack configurations. The results are discussed with special attention to effects induced by crack interaction.

## PROBLEM FORMULATION AND BIE

Consider an infinite, homogeneous, isotropic and linearly elastic solid containing two parallel cracks as depicted in Fig. 1a. The crack faces $A_1^{\pm}$, $A_2^{\pm}$ are loaded by an impact $-\sigma_{i3}^{\text{in}}$ induced for example by an incident transient wave. The main interest is directed to the dynamic K-factors along the crack fronts.

Following Zhang (1991) and Zhang & Gross (1993a,b), the problem can be reduced to the following non-hypersingular time-domain BIEs for the unknown crack opening displacements (CODs) $\triangle u_i(\mathbf{y},\tau)$

$$\int_{A_1^+ + A_2^+} \int_0^t \Big\{ E_{p3kl}\epsilon_{r3t}\epsilon_{rlj}\sigma_{ijk}^G(\mathbf{x},t;\mathbf{y},\tau)\triangle u_{i,t}(\mathbf{y},\tau) + E_{p3k3}\rho u_{ik}^G(\mathbf{x},t;\mathbf{y},\tau)\triangle\ddot{u}_i(\mathbf{y},\tau)\Big\}\mathrm{d}\tau\mathrm{d}S = \sigma_{p3}^{\text{in}}(\mathbf{x},t)\,, \quad \mathbf{x}\in A_1^+ + A_2^+\,, \quad (1)$$

where $\epsilon_{rst}$ is the permutation tensor and $E_{pqkl}$ is the elasticity tensor, which for an isotropic material is given by

$$E_{pqkl} = \lambda\delta_{pq}\delta_{kl} + \mu(\delta_{pk}\delta_{ql} + \delta_{pl}\delta_{qk})\,, \quad (2)$$

with $\lambda$ and $\mu$ being the Lamé constants. In Eqs. (1) and (2) $\rho$ is the mass density, $\delta_{pq}$ the Kronecker delta, $u_{ik}^G$ and $\sigma_{ijk}^G$ are the displacement and stress Green's functions of the uncracked full-space, see Zhang & Gross (1993a,b). The CODs are defined by

$$\triangle u_i(\mathbf{y},\tau) = u_i(\mathbf{y}\in A^+,\tau) - u_i(\mathbf{y}\in A^-,\tau)\,. \quad (3)$$

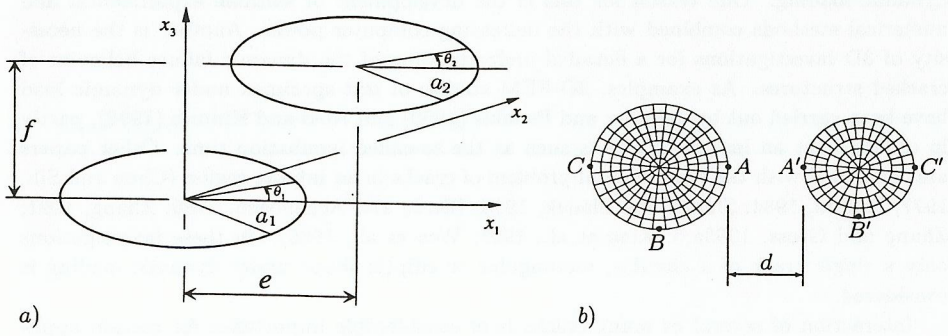


Figure 1: a) Parallel penny-shaped cracks b) BIEM-mesh



Once they are calculated by solving the integral equations, all quantities at an arbitrary internal point of the solid, such as the displacements, the strains and the stresses, can be determined by use of the corresponding representation formulas for these quantities. The dynamic K-factors along the crack fronts also can easily be determined from the standard relations (here for a penny-shaped crack of radius $a$)

$$\left\{\begin{array}{c} K_I(\theta,t) \\ K_{II}(\theta,t) \\ K_{III}(\theta,t) \end{array}\right\} = \frac{\mu\sqrt{2\pi}}{4(1-\nu)} \lim_{r\to a} \frac{1}{\sqrt{a-r}} \left\{\begin{array}{c} \triangle u_3(r,\theta,t) \\ \triangle u_r(r,\theta,t) \\ (1-\nu)\triangle u_\theta(r,\theta,t) \end{array}\right\}. \quad (4)$$

where $\triangle u_r$ and $\triangle u_\theta$ are the CODs in the polar coordinate system and $\nu$ is Poisson's ratio.

## NUMERICAL SOLUTION PROCEDURE

The BIEs (1) are solved numerically by use of a collocation method in conjunction with a time-stepping scheme. Applying the procedure described by Zhang & Gross (1993a,b) the following time-stepping scheme for calculating the discrete COD-values is obtained

$$(\triangle u_i)_e^1 = \sum_{d=1}^{E} (A_{ip;ed}^1)^{-1} \sigma_{p3}^{\text{in}}(\mathbf{x}^d,t_1)\,, \quad (5)$$

$$(\triangle u_i)_e^q = \sum_{d=1}^{E} (A_{ip;ed}^1)^{-1} \left[\sigma_{p3}^{\text{in}}(\mathbf{x}^d,t_q) - \sum_{s=1}^{q-1}\sum_{f=1}^{E} A_{kp;df}^{q-s+1}(\triangle u_k)_f^s\right], \quad (q\geq 2)\,, \quad (6)$$

where $q = m-n+1$, $A_{ip;ed}^q = A_{ip;ed}^{mn}(m\geq n)$ and $A_{ip;ed}^{mn}$ takes the form

$$\begin{aligned} A_{ip;ed}^{mn} = {} & E_{p3kl}\Big\{\epsilon_{r3\alpha}\epsilon_{rlj}\int_{A_e^+} \Sigma_{ijk}(\mathbf{x}^d,t_m;\mathbf{y},t_n)[g_{,\alpha}(\mathbf{y}) - g_{,\alpha}(\mathbf{x}^d)]\mathrm{d}S \\ & + \epsilon_{r3\alpha}\epsilon_{rlj}E_{ijuv}g_{,\alpha}(\mathbf{x}^d)\int_{\partial A_e^+} U_{uk}(\mathbf{x}^d,t_m;\mathbf{y},t_n)m_v(\mathbf{y})\mathrm{d}s \\ & - \epsilon_{r3\alpha}\epsilon_{rlj}\int_{\partial A_e^+} \Sigma_{ijk}(\mathbf{x}^d,t_m;\mathbf{y},t_n)g(\mathbf{y})m_\alpha(\mathbf{y})\mathrm{d}s\Big\} \\ & + \rho E_{p3k3}\int_{A_e^+} V_{ik}(\mathbf{x}^d,t_m;\mathbf{y},t_n)g(\mathbf{y})\mathrm{d}S\,, \end{aligned} \quad (7)$$

with

$$U_{ik}(\mathbf{x}^d,t_m;\mathbf{y},t_n) = \frac{1}{4\pi\rho r}\{(3r_{,i}r_{,k}-\delta_{ik})F + r_{,i}r_{,k}G_L/c_L^2 + (\delta_{ik}-r_{,i}r_{,k})G_T/c_T^2\}\,, \quad (8)$$

$$V_{ik}(\mathbf{x}^d, t_m; \mathbf{y}, t_n) = \frac{1}{\triangle t}\{u^G_{ik}(\mathbf{x}^d, t_m; \mathbf{y}, t_{n-1}) - 2u^G_{ik}(\mathbf{x}^d, t_m; \mathbf{y}, t_n) + u^G_{ik}(\mathbf{x}^d, t_m; \mathbf{y}, t_{n+1})\}\,, \tag{9}$$

$$\Sigma_{ijk}(\mathbf{x}^d, t_m; \mathbf{y}, t_n) = -\frac{1}{4\pi r^2}\{6A_{ijk}c_T^2 F + 2\frac{r}{c_T}r_{,i}r_{,j}r_{,k}(H_T - H_L/\kappa^3) + 2B_{ijk}(G_T - G_L/\kappa^2) - \delta_{ij}r_{,k}(1-2\kappa^{-2})(G_L + rH_L/c_L) - (\delta_{ik}r_{,j} + \delta_{jk}r_{,i})(G_T + rH_T/c_T)\}\,. \tag{10}$$

$A_e^+$ is the area of the $e$th element with boundary $\partial A_e^+$, and $\mathbf{m} = \mathbf{t} \times \mathbf{n}$ is a unit vector normal to $\partial A_e^+$ tangent to $A_e^+$ and pointing outward, and $\mathbf{t}$ is the unit tangent vector to $\partial A_e^+$. Furthermore, $\kappa = c_L/c_T$ with

$$c_L = \sqrt{\frac{\lambda + 2\mu}{\rho}}\,, \qquad c_T = \sqrt{\frac{\mu}{\rho}}\,, \tag{11}$$

being the dilatational and shear wave velocity respectively. The auxiliary functions $F$, $G_\xi$, $H_\xi$ ($\xi = L, T$) and abbreviations $A_{ijk}$, $B_{ijk}$ can be found in Zhang & Gross (1993a,b). In (7) only a weak singularity arises which provides no difficulty for numerical integrations.

The BIEM-mesh used in calculations for penny-shaped cracks is shown in Fig. 1b. In most cases a total of 336 elements has been used. For elements away from the crack fronts, the shape function $g(\mathbf{y})$ is taken to be unity (constant elements), while for elements in the vicinity of the crack front, a specially designed 'square-root' crack-tip shape function is applied to describe the proper behavior of the crack opening displacement and its derivatives at the crack front. In order to obtain better results the time step $\triangle t$ should be selected such that the dynamic K-factors can best be fit within some particular range of time $t$, including $t \to \infty$, the static case. In this investigations the time step has been chosen as $c_T\triangle t/a_1 = 0.1405 \ldots 0.1425$.

## RESULTS AND DISCUSSION

Calculations have been carried out for two coplanar cracks ($f = 0$), two stacked cracks ($e = 0$) and two arbitrarily located cracks ($f \neq 0$, $e \neq 0$) under impact loads. For the sake of brevity, results only for normal impact $\sigma H(t)$ are presented, with $H(t)$ being the Heaviside step function. Poisson's ratio of the material is taken as $\nu = 0.29$ or $\nu = 0.3$ in order to compare the stationary K-factors computed in this paper with static K-factors available in the literature. For convenience, the following normalization is introduced

$$\bar{K}_I(\theta, t) = \frac{K_I(\theta, t)}{K_1}\,, \qquad \bar{K}_{II}(\theta, t) = \frac{K_{II}(\theta, t)}{K_2}\,, \qquad \bar{K}_{III}(\theta, t) = \frac{K_{III}(\theta, t)}{K_3}\,, \tag{12}$$

where

$$K_1 = 2\sigma\sqrt{\frac{a_i}{\pi}}\,, \qquad K_2 = \frac{1-2\nu}{(2-\nu)(1-\nu)}2\sigma\sqrt{\frac{a_i}{\pi}}\,, \qquad K_3 = -\frac{1-2\nu}{2-\nu}2\sigma\sqrt{\frac{a_i}{\pi}}\,. \tag{13}$$



*Coplanar Penny-Shaped Cracks*

For two coplanar penny-shaped cracks under normal impact, the only nonzero stress intensity factor is $K_I$. First, cracks of same radii $a_1 = a_2 = a$ are considered. Due to the symmetry, the $K$-factor distributions along the crack fonts of both cracks are the same: $K_I(\theta_1, t) = K_I(\theta_2, t)$ with $\theta_2 = 180° - \theta_1$. In Fig. 2 the normalized $K_I$-factor is depicted versus dimensionless time $c_T t/a$ for two different crack distances $e/a$. The figures show the general time-behaviour of the dynamic K-factors: immediately after the impact the K-factor increases rapidly with time $t$. After reaching a maximum, $K_I$ decreases, then increases again and oscillates around the corresponding static value. When $t$ tends to infinity, the dynamic K-factor approaches to its static stress intensity factor.

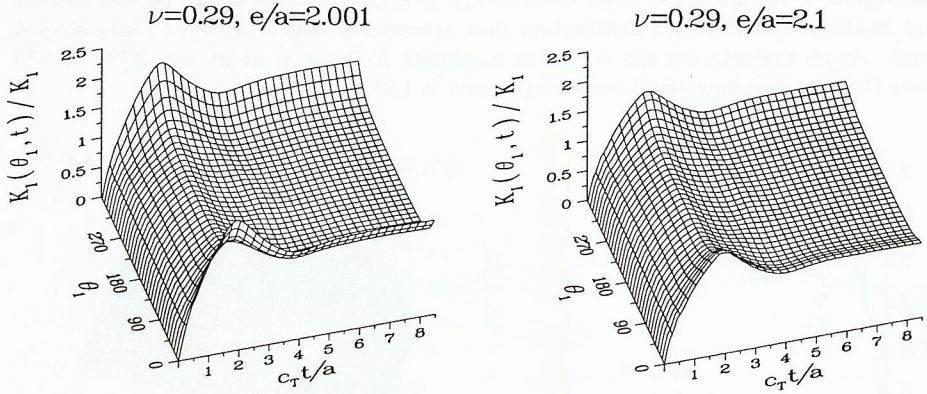


Figure 2: $K_I$-factors for coplanar cracks with a same radius

From the computations it can be seen that $K_I(\theta_1, t)$ at the crack tip point $A$ ($\theta_1 = 0°$) is larger than that at any other point along the crack front. To present the interaction effect more clearly, Table 1 shows the maximum K-factors, the 'stationary' K-factors (at $c_T t_{st}/a = 8.55$) and the corresponding static K-factors at the three crack front points $A$, $B$, $C$ ($\theta_1 = 0°, 90°, 180°$). From the results it is observed that the 'stationary' stress intensity factors and static stress intensity factors are in good agreement for $e/a \geq 2.1$. The deviations in these cases are less than 2.5% what also can be taken as an indicator for the accuracy of the calculations. When the distance between the two cracks decreases the deviations between the 'stationary' and static K-factors become larger and larger, particularly for the two nearest crack front points $A$. For $e/a = 2.2, 2.1, 2.01, 2.001$, the deviations at $A$ are 0.34%, 2.48%, 18.5% and 37.8%, respectively. But it also interesting to note that for all results within the range of $22.5° \leq \theta_1 \leq 337.5°$, no matter how close the two cracks are, the deviations between the 'stationary' and static K-factors are less than 2.5%. This is also true for the crack distance $e/a = 2.0005$ whose numerical results are omitted here for the sake of brevity. On the other hand, notable numerical errors in

Table 1: $K$-factors of two coplanar penny-shaped cracks

| $e/a$ | 2.001 | | | 2.01 | | | 2.1 | | | 2.2 | | |
|---|---|---|---|---|---|---|---|---|---|---|---|---|
| Point | $A$ | $B$ | $C$ | $A$ | $B$ | $C$ | $A$ | $B$ | $C$ | $A$ | $B$ | $C$ |
| $\bar{K}_I^{max}$ | 2.19 | 1.34 | 1.30 | 2.09 | 1.33 | 1.30 | 1.70 | 1.33 | 1.30 | 1.55 | 1.32 | 1.30 |
| $\bar{K}_I(t_{st})$ | 1.59 | 1.05 | 1.03 | 1.52 | 1.05 | 1.03 | 1.26 | 1.04 | 1.03 | 1.16 | 1.04 | 1.02 |
| $\bar{K}_I^{static}$ * | 2.56 | 1.04 | 1.02 | 1.86 | 1.04 | 1.02 | 1.29 | 1.03 | 1.02 | 1.17 | 1.02 | 1.01 |

* normalized static K-factors given by Fabrikant (1987).

the computations appear along the crack fronts within the range of $|\theta_1| < 22.5°$ for closely coplanar cracks. Reason is the strong crack interaction accompanied by high $K$-gradients along the front. The errors can only be avoided by increasing the number of elements in this region. With increasing crack distance $e/a \geq 2.2$, interaction effects become smaller and smaller. The $K$-factor distribution then approaches that of a single penny-shaped crack. As an example, for $e/a = 0.5$ the maximum $K$-factor at point $A$ is $\bar{K}_I^{max} = 1.39$ while the corresponding result for a single crack is 1.31.

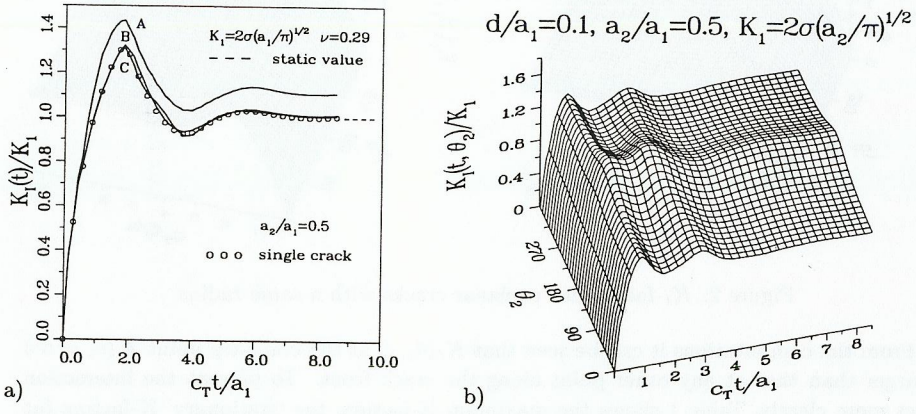


Figure 3: Coplanar cracks with different radii a) large crack b) small crack

Now the radius $a_1$ of the first crack and the crackfront distance $d$ is held constant ($d/a_1 = 0.1$) while the second crack is taken as smaller and smaller. Results for $a_2/a_1 = 0.5$ are plotted in Fig. 3 for the large and the small crack. The large crack observes an interaction with the smaller one only in the crackfront vicinity of point $A$. The peak value there is $\bar{K}_I^{max} = 1.43$; along the crackfront farer away from $A$ (e.g. points $B$, $C$) the $K_I(t)$-curves are essentially the same as for a single crack. The interaction effect is more pronounced at the small crack. A second peak value now developes at $c_T t/a_1 \approx 3$ which can be explained by the emmitted stress peak from the large crack and the accompanied wave speeds and travel distances: The farther a crackfront point is located from the large crack the later the second peak evolves. The second peak partly might be higher as the



first one. Indeed the maximum $K$-factor at the small crack arises at the second peak at point $A'$: $\bar{K}_I^{max} = 1.67$ (note, the $K$-factor is normalized with its own static single crack value)

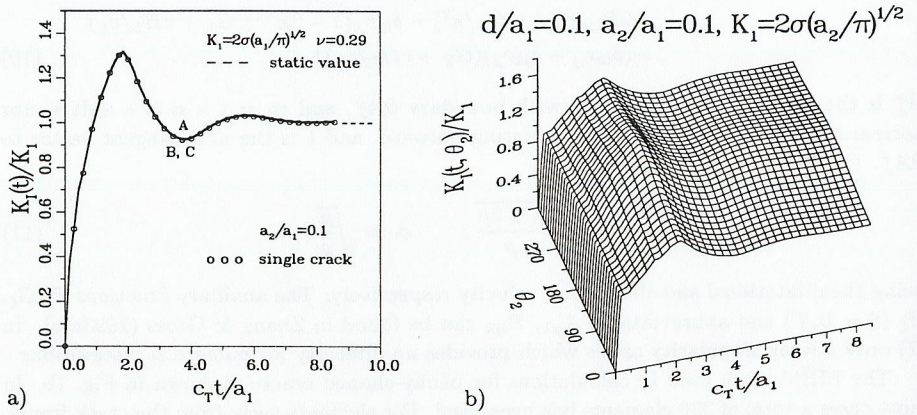


Figure 4: Macro-micro interaction of coplanar cracks a) large crack b) small crack

$K$-factor distributions for $a_2/a_1 = 0.1$ are shown in Fig. 4. This case can be regarded as a macro-microcrack interaction. The large crack now is neglegible influenced by the microcrack. Within the accuracy of the computation, the $K$-curves for the points $A$, $B$ and $C$ coincide with the corresponding curve of a single crack. The stress intensity distribution of the microcrack is mainly determined by the macrocrack. The first peak has vanished and only the second peak, induced by the macrocrack, appears at time $c_T t/a_1 \approx 3$, with a maximum value of $\bar{K}_I^{max} = 1.67$ at point $A'$. The 'stationary' value at this point is $\bar{K}_I(t_{st}) = 1.35$, which approaches the corresponding static value.

*Two Stacked Penny-Shaped Cracks*

In this case $K_{III} = 0$ and two modes with the stress intensity factors $K_I$, $K_{II}$ are present, which due to the axisymmetry are constant along the crack fronts. In addition, the $K$-factors for both cracks are the same if the radii are equal ($a_1 = a_2 = a$) and the cracks are impacted at the same time. Fig. 5 shows results for this special case for different distances $f$. The dashed lines stand for the corresponding static K-factors given by Isida et al. (1985), Murakami (1987) and Kachanov & Laures (1989). It can be seen that before the disturbing waves from one crack arrives at the other crack, as expected, the dynamic $K_I$-factors for the two crack problem are as same as those for the corresponding single crack problem. When the wave front (essentially pressure) from the one crack reaches the other crack front, it reduces the $K_I$-factors, compared with the corresponding single crack problem. After the first peak they oscillate around the corresponding static values and when $t$ tends to infinity, they approach to their static K-factors. The different frequency

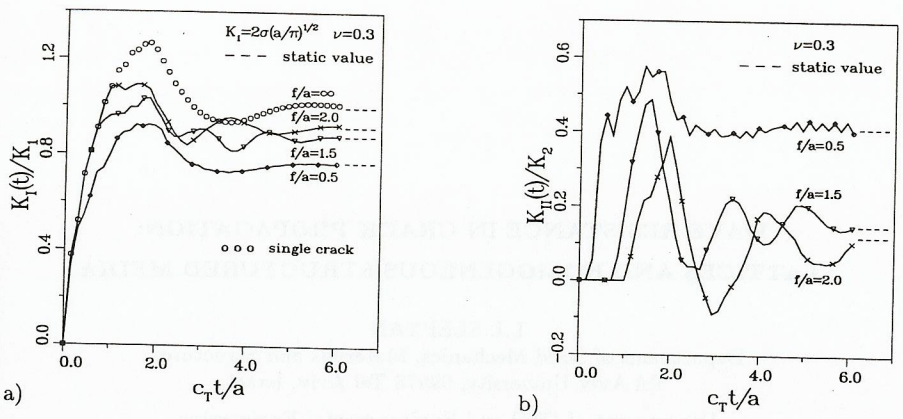


Figure 5: Two stacked cracks with a same radius

of the oscillations, clearly seen for $f/a = 2.0$ and $f/a = 1.5$ can simply be explained by the multiple reflections (compression - tension) of waves running between the two cracks.

The dynamic $K_{II}$-factors are zero before the wave front from the one crack arrives at the other one. Then this interaction induced wave loading leads to a rapid increase of $K_{II}$. After reaching a maximum, they decrease and increase again, oscillating around the corresponding static values and approaching them when $t$ tends to infinity. The different oscillation frequency again is explained by the waves running between the two cracks The computations show that the interaction effect on $K_I$ and $K_{II}$ decreases with increasing crack distance $f$. For $f/a \geq 10$ the effect almost vanishes and the two crack problem can be solved adequately by the corresponding single crack problem.

*Two Arbitrarily Located Penny-Shaped Cracks*

Now all three modes are present. On account of the symmetry, the distributions of $K_I$, $K_{II}$ and $K_{III}$ at both cracks are equal for $a_1 = a_2 = a$ and the same impact time. As an example, Fig. 6 shows the result for the geometry parameters $e/a = 1$ and $f/a = 1$. The time behaviour of $K_I$ and $K_{II}$, to a certain extent, is similar to that for the stacked cracks. Remarkable is the relatively high mode III peak value of $\bar{K}_{III}^{max} = 0.6$ and the zero $K_{III}$ at $\theta = \pi$, the last due to the symmetry. It also shall be noted that the maximum interaction effects for mode I and for mode II, mode III are shiftet against each other along the crack front by $\pi/2$. Again, the interaction effects almost vanish if one of the two crack distance parameters is high enough, e.g. for $f/a = 1.0$, $e/a = 3.0$.

Table 2 shows the maximum K-factors, the 'stationary' K-factors and the static K-factors at the crack front points $A$, $B$, $C$. At large time $t$, good agreement between the 'stationary' and the static stress intensity factors can be observed. For all computations the deviation was always less than 1%.



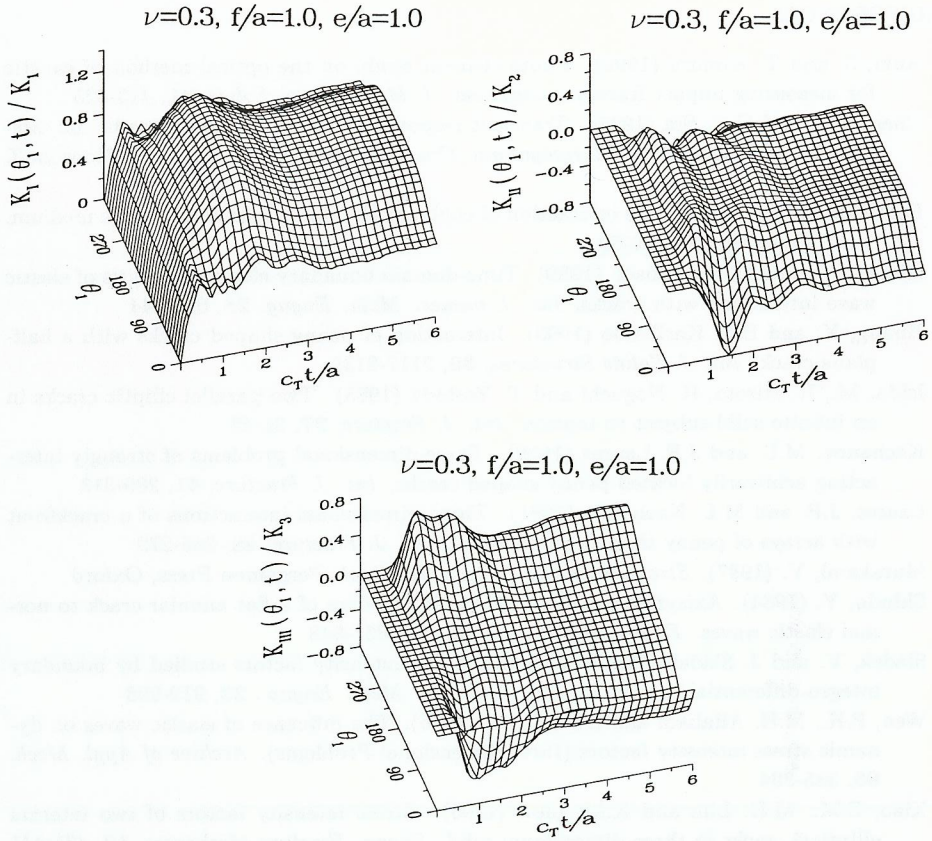


Figure 6: Two arbitrarily located cracks with a same radius

Table 2: $K$-factors for two arbitrarily located penny-shaped cracks, $f/a = 1$

| $e/a$ | 1.0 | | | 2.0 | | | 3.0 | | |
|---|---|---|---|---|---|---|---|---|---|
| Point | $A$ | $B$ | $C$ | $A$ | $B$ | $C$ | $A$ | $B$ | $C$ |
| $\bar{K}_I^{max}$ | 0.85 | 1.23 | 1.28 | 1.26 | 1.31 | 1.26 | 1.31 | 1.26 | 1.26 |
| $\bar{K}_I(t_{st} = 6.063a/c_T)$ | 0.68 | 0.98 | 1.02 | 0.99 | 1.04 | 1.03 | 1.04 | 1.02 | 1.01 |
| $\bar{K}_I^{static\,*}$ | 0.66 | - | - | 0.97 | - | - | 1.02 | - | - |
| $\bar{K}_I^{static\,**}$ | 0.66 | - | 1.02 | 0.97 | - | 1.02 | 1.02 | - | 1.01 |

* normalized static K-factors given by Kachanov & Laures (1989).

** normalized static K-factors given by Isida et al. (1985) and Murakami (1987).

REFERENCES

Aoki, S. and T. Kimura (1993). Finite element study on the optical method of caustic for measuring impact fracture toughness. *J. Mech. Phys. Solids,* **41**, 413-425

Chen, E.P. and G.C. Sih (1977). Transient response of cracks to impact loads. In: *Mechanics of Fracture IV: Elastodynamic Crack problems* (G.C. Sih, ed.), Noordhoff, Leyden

Fabrikant, V.I. (1987). Close interaction of coplanar circular cracks in an elastic medium. *Acta Mechanica,* **67**, 39-59

Hirose, S. and J.D. Achenbach (1989). Time-domain boundary element analysis of elastic wave interaction with cracks. *Int. J. numer. Meth. Engng.* **28**, 629-644

Huang, X. and B.L. Karihaloo (1993). Interaction of penny shaped cracks with a half-plane crack. *Int. J. Solids Structures,* **30**, 2117-2139

Isida, M., K. Hirota, H. Noguchi and T. Yoshida (1985). Two parallel elliptic cracks in an infinite solid subject to tension. *Int. J. Fracture,* **27**, 31-48

Kachanov, M.L. and J.P. Laures (1989). Three-dimensional problems of strongly interacting arbitrarily located penny shaped cracks. *Int. J. Fracture,* **41**, 289-313

Laures, J.P. and M.L. Kachanov (1991). Three dimensional interactions of a crackfront with arrays of penny shaped microcracks. *Int. J. Fracture,* **48**, 255-279

Murakami, Y. (1987). *Stress Intensity Factors Handbook*, Pergamon Press, Oxford

Shindo, Y. (1984). Axisymmetric elastodynamic response of a flat annular crack to normal elastic waves. *Engng. Fracture Mech.,* **19**, 837-848

Sládek, V. and J. Sládek (1986). Dynamic stress intensity factors studied by boundary integro-differential equations. *Int. J. numer. Meth. Engng.,* **23**, 919-928

Wen, P.H., M.H. Aliabadi and D.P. Rooke (1996). The influence of elastic waves on dynamic stress intensity factors (three dimensional Problems). *Archive of Appl. Mech.* **66**, 385-394

Xiao, Z.M., M.K. Lim and K.M. Liew (1995). Stress intensity factors of two internal elliptical cracks in three-dimensional solid. *Engng. Fracture Mechanics,* **50**, 431-441

Zehnder, A.T. and A.J. Rosakis (1990). Three-dimensional effects near a crack tip in a ductile three-point bend specimen, II. An experimental investigation using interferometry and caustics. *J. Appl. Mech.* **57**, 618-626

Zhang, Ch. (1991). A novel derivation of non-hypersingular time-domain BIEs for transient elastodynamic crack analysis. *Int. J. Solids Structures,* **28**, 267-281

Zhang, Ch. and D. Gross (1993a). A non-hypersingular time-domain BIEM for 3-D transient elastodynamic crack analysis. *Int. J. Numer. Meth. Engng.,* **36**, 2997-3017

Zhang, Ch. and D. Gross (1993b). Transient elastodynamic analysis of a penny-shaped crack. *Engng. Fracture Mech.,* **46**, 641-654